DALTON
FULL PAPER

Synthesis, structure, redox activity and spectroscopic properties of ruthenium(II) complexes with 3,5-bis(benzothiazol-2-yl)pyrazole, 3,5-bis(benzimidazol-2-yl)pyrazole and 2,2′-bipyridine as co-ligands

Sujoy Baitalik,[a] Ulrich Flörke[b] and Kamalaksha Nag*†[a]

[a] *Department of Inorganic Chemistry, Indian Association for the Cultivation of Science, Jadavpur, Calcutta 700 032, India. E-mail: ickn@mahendra.iacs.res.in*
[b] *Anorganische und Analytische Chemie der Universität Gesamthochschule Paderborn, D-33098, Paderborn, Germany*

Received 8th September 1998, Accepted 10th December 1998

Ruthenium(II) complexes of composition $[(bipy)_2Ru(Hpzbzth)][ClO_4]_2\cdot 3H_2O$ **1**, $[(bipy)_2Ru(pzbzth)][ClO_4]\cdot 2H_2O$ **2**, $[(bipy)_2Ru(pzbzth)Ru(bipy)_2][ClO_4]_3\cdot H_2O$ **3**, $[(bipy)_2Ru(H_3pzbzim)][ClO_4]_2\cdot 2H_2O$ **4** and $[(bipy)_2Ru(Hpzbzim)]\cdot 2H_2O$ **5**, where Hpzbzth = 3,5-bis(benzthiazol-2-yl)pyrazole, H_3pzbzim = 3,5-bis(benzimidazol-2-yl)pyrazole and bipy = 2,2′-bipyridine, have been synthesized and characterized. The crystal structure of **3**, in which the two metal centres are bridged by the pyrazolate moiety of the pzbzth anion, has been determined. The two RuN_6 chromophores in this complex are separated by 4.723(3) Å. From the significant down-field shift of the pyrazolate CH proton in **3** (8.92 ppm) with respect to **1** (7.78 ppm) and **4** (7.82 ppm), the involvement of S · · · H(C) · · · S type interaction in **3** has been proposed. The equilibrium constants of the species involving dissociation of the NH protons of the bridging ligand and the change in the oxidation state of ruthenium from +2 to +3 have been determined in acetonitrile–water (3 : 2) by cyclic voltammetric and spectrophotometric methods. Redox titrations of complexes **1**, **3** and **4** by cerium(IV) have revealed that the disappearence of the metal-to-ligand charge transfer band is accompanied by the appearence of the ligand-to-metal charge transfer band at higher wavelengths. In the case of **3**, when 1 equivalent of cerium(IV) is added, the mixed-valence $Ru^{II}Ru^{III}$ species is generated which exhibits an absorption maximum at 950 nm due to the intervalence-transfer transition. The luminescence spectral behaviour of complexes **1**–**4** has been examined in methanol–ethanol (1 : 4) solution (at 300 K) as well as in glassy state (at 77 K).

Cooperative interactions between metal centres in heterocyclic ligand-based di- and multi-nuclear ruthenium(II) and osmium(II) complexes give rise to properties[1–5] that are useful for constructing photomolecular devices. The redox activities and the ground and excited state properties of such complexes are strongly influenced by the nature of the bridging ligand mediating metal–metal interactions. The specific role of a bridging ligand is governed by several factors, *viz.* the donor and acceptor properties of the coordination sites, the length and rigidity of spacers, the presence or absence of conjugated bonds, the orientation of the substituents and the scope of manipulating ligand charge. To be effective, the molecular orbitals of the bridging ligand should be symmetry- and energy-matched to interact with the donor and acceptor orbitals of the metal centres.

Two types of bridging ligands are generally used to assemble polypyridyl ruthenium(II) and osmium(II) building blocks.[1–7] The majority of these ligands are neutral and electron-poor and they are oligomeric pyridine, pyrazine or pyrimidine derivatives. They mediate intermetallic interactions through low-lying π* orbitals (LUMOs) by invoking electron transfer superexchange mechanism. On the other hand, electron-rich bridging ligands such as 3,5-bis(pyridin-2-yl)-1,2,4-triazolate (1−),[8] 3,5-bis(pyrazin-2-yl)-1,2,4-triazolate (1−),[9] 2,2′-diimidazolate (2−),[10] and 2,2′-dibenzimidazolate (2−)[10,11] assist metal–metal coupling *via* hole transfer mechanism, taking advantage of relatively high-lying filled molecular orbitals (HOMOs). Between these two types, there are some ligands which are electrically neutral but can be made anionic on complex formation by deprotonating one or more dissociable NH protons present. Complexes derived from ligands of this sort, *viz*. 2,2′-bis-(2-pyridyl)dibenzimidazole,[12] 2,6-bis(2′-pyridyl)benzdiimidazole,[13] 2,2′-bis(2-benzimidazolyl)-4,4′-bipyridine,[14] 1,3,5-tris-[5-(pyridin-2-yl)-1,2,4-triazol-3-yl] benzene[15] and 1,3,5-tris[5-(pyrazin-2-yl)-1,2,4-triazol-3-yl]benzene[15] have also received considerable attention.

We report here the synthesis, structural characterization, redox activities, and absorption and emission spectral characteristics of the ruthenium(II) mixed-chelates $[Ru(Hpzbzth)(bipy)_2]^{2+}$ and $[(bipy)_2Ru(pzbzth)Ru(bipy)_2]^{3+}$ derived from 3,5-bis(benzothiazol-2-yl)pyrazole (Hpzbzth) and 2,2′-bipyridine (bipy). The pH-dependent electro-protic equilibria, the transformation of MLCT to LMCT absorptions during oxidative titrations of $[Ru(Hpzbzth)(bipy)_2]^{2+}$ and $[Ru(H_3pzbzim)(bipy)_2]^{2+}$ (where H_3pzbzim = 3,5-bis(benzimidazol-2-yl)pyrazole) and the generation of the mixed-valence $[(bipy)_2Ru^{II}(pzbzth)Ru^{III}(bipy)_2]^{4+}$ species in solution are also reported in this study.

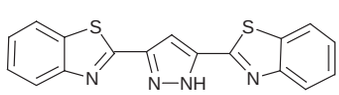

Hpzbzth

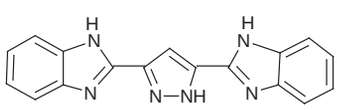

H_3pzbzim

Experimental

Materials

All chemicals were obtained from commercial sources and used as received. Solvents were purified and dried according to

standard methods.[16] 3,5-Pyrazole dicarboxylic acid monohydrate[17] and $[Ru(bipy)_2Cl_2]\cdot 2H_2O$[18] were prepared by the literature methods. Robinson-Britton buffer solutions[19] of pH range 1–12 were used.

Preparation of the ligands

A modified version[20] of the Phillips method[21] was used to prepare the ligands Hpzbzth and H_3pzbzim.

Hpzbzth. A mixture of pyrazole-3,5-dicarboxylic acid monohydrate (3.4 g, 20 mmol) and *o*-aminothiophenol (5.0 g, 40 mmol) in syrupy phosphoric acid (40 cm^3) was heated at 140 °C for 3 h under nitrogen atmosphere. The resulting light yellow liquid was poured into crushed ice (*ca.* 1 dm^3) and the mixture was carefully neutralized with a KOH solution (3 mol dm^{-3}). A greenish yellow precipitate thus obtained was filtered off, washed several times with water and dried over P_2O_5 under vacuum. The product on recrystallization from acetone gave yellowish green platelets; yield 2.0 g (30%), mp >250 °C (Found: C, 61.2; H, 3.1; N, 16.7. $C_{17}H_{10}N_4S_2$ requires : C, 61.1; H, 3.0; N, 16.75%). ν/cm^{-1}(KBr) : 3100, 1600, 1560, 1480, 1450, 1430, 1320, 1240, 1200, 1180, 950, 930, 810, 750, 720, 700 cm^{-1}.

H_3pzbzim. A mixture of *o*-phenylenediamine (4.5 g, 41.5 mmol) and pyrazole-3,5-dicarboxylic acid monohydrate (3.4 g, 20 mmol) and polyphosphoric acid (40 cm^3) was heated at 200 °C for 4 h. The deep blue viscous solution that formed was poured into crushed ice (*ca.* 1 dm^3). A blue precipitate thus obtained was filtered, washed with water, followed by dilute aqueous ammonia and again water. During this process the residue changed to light pink. This was dissolved in the minimum volume of hot (90 °C) *N*,*N*′-dimethylformamide (DMF), treated with a small amount of activated charcoal, and filtered. To the filtrate water was slowly added when the product separated out as an off-white solid, which was recrystallized from DMF–H_2O; yield 2.7 g (40%), mp >250 °C (Found: C, 67.7; H, 3.95; N, 27.75. $C_{17}H_{12}N_6$ requires: C, 68.0; H, 4.0; N, 28.0%). ν/cm^{-1}(KBr): 3050, 2800, 1655, 1615, 1570, 1510, 1465, 1430, 1390, 1350, 1270, 1230, 1210, 1100, 1015, 960, 760, 750 cm^{-1}.

Preparation of the complexes

CAUTION: All the perchlorate salts reported in this study are potentially explosive and therefore should be handled with care.

$[(bipy)_2Ru(Hpzbzth)][ClO_4]_2\cdot 3H_2O$ 1. A solution of $[(bipy)_2Ru(EtOH)_2][ClO_4]_2$ was prepared by stirring a mixture of $[(bipy)_2RuCl_2]$ (0.52 g, 1 mmol) and $AgClO_4$ (0.42 g, 2 mmol) in ethanol (50 cm^3) at room temperature for 2 h, followed by removal of AgCl precipitated. To the filtrate solid Hpzbzth (0.41 g, 1.25 mmol) and 0.5 cm^3 of $HClO_4$ (1 mmol dm^{-3}) were added. The mixture was stirred and heated under reflux for 10 h, after which it was cooled to room temperature and the unreacted ligand was removed by filtration. The filtrate was concentrated to *ca.* 20 cm^3 and kept overnight in a refrigerator. The orange crystals that deposited were filtered and recrystallized from methanol–water (5 : 1) containing two drops of $HClO_4$ (1 mmol dm^{-3}); yield 0.6 g (60%) (Found: C, 44.3; H, 2.9; N, 11.1. $C_{37}H_{32}Cl_2N_8O_{11}RuS_2$ requires : C, 44.4; H, 3.2; N, 11.2%). ν/cm^{-1}(KBr) 3400(br), 1605, 1540, 1470, 1450, 1425, 1320, 1100(br), 975, 760, 730 and 625 cm^{-1}.

$[(bipy)_2Ru(pzbzth)][ClO_4]\cdot 2H_2O$ 2. A methanol solution (20 cm^3) of **1** (0.25 g, 0.25 mmol) on treatment with triethylamine (40 mm^3, 0.3 mmol) changed immediately from red–orange to deep red. On concentration of the solution (*ca.* 3 cm^3) vermilion microcrystals deposited. These were collected by filtration and recrystallized from a methanol–ethanol (1 : 1) mixture; yield 0.18 g (82%) (Found: C, 50.2; H, 3.0; N, 12.5. $C_{37}H_{29}ClN_8O_6RuS_2$ requires : C, 50.35; H, 3.3; N, 12.7%). ν/cm^{-1}(KBr) 3400 (br), 1535, 1470, 1450, 1425, 1320, 1250, 1200, 1125, 1100 (br), 970, 930, 770, 730 and 630 cm^{-1}. ^{1}H NMR $[(CD_3)_2SO]$: δ 6.10 (1H, d), 7.17 (1H, t), 7.33 (1H, t), 7.38–7.58 (6H, m), 7.63 (1H, t), 7.74 (1H, d), 7.78 (1H, s), 7.90 (1H, d), 7.96 (1H, d), 8.01–8.22 (7H, m), 8.74 (2H, d), 8.79 (1H, d), 8.84 (1H, d).

$[(bipy)_2Ru(pzbzth)Ru(bipy)_2][ClO_4]_3\cdot H_2O$ 3. To an ethanol solution (25 cm^3) of **1** (0.25 g, 0.20 mmol) was added a second ethanol solution (10 cm^3) of $[(bipy)_2Ru(EtOH)_2][ClO_4]_2$ (obtained from 0.13 g, 0.25 mmol of $[Ru(bipy)_2Cl_2]$) followed by triethylamine (35 mm^3, 0.25 mmol). The solution was refluxed for 1 h and then concentrated on a rotary evaporator to obtain the deep red microcrystalline product. This was recrystallized from methanol–acetonitrile (1 : 1); yield 0.32 g (87%) (Found: C, 46.1; H, 3.05; N, 11.45. $C_{57}H_{34}Cl_3N_{12}O_{13}Ru_2S_2$ requires: C, 46.35; H, 2.9; N, 11.4%). ν/cm^{-1}(KBr) 3400 (br), 1600, 1550, 1455, 1440, 1415, 1380, 1320, 1265, 1235, 1100 (br), 980, 760, 730 and 625 cm^{-1}. ^{1}H NMR $[(CD_3)_2SO]$: δ 5.65 (2H, d, 8.5 Hz), 6.33 (2H, d, 5.1 Hz), 6.85 (2H, d, 5.3 Hz), 6.87 (2H, t, 7.0 Hz), 7.00 (2H, t, 7.7 Hz), 7.36 (6H, t, 7.7 Hz), 7.52 (2H, d, 5.0 Hz), 7.55 (2H, t, 6.8 Hz), 7.65 (2H, t, 7.9 Hz), 8.00 (6H, m, 8.1 Hz), 8.11 (2H, t, 7.0 Hz), 8.26 (4 h, d, 7.2 Hz), 8.40 (2H, d, 8.2 Hz), 8.46 (4 H, d, 8.3 Hz).

$[(bipy)_2Ru(H_3pzbzim)][ClO_4]_2\cdot 2H_2O$ 4. A mixture of $[Ru(bipy)_2Cl_2]\cdot 2H_2O$ (0.26 g, 0.5 mmol) and H_3pzbzim (0.3 g, 1 mmol) in 50 cm^3 of ethanol-water (1 : 1) was heated under reflux with constant stirring for 24 h. After removal of the unreacted ligand, the orange-red filtrate was rotary-evaporated to *ca.* 20 cm^3 and to it was then added an aqueous solution (5 cm^3) of $NaClO_4$ (1 g). The product that separated was filtered and recrystallized from methanol–water (3 : 1) containing a few drops of $HClO_4$ (1 mmol dm^{-3}); yield 0.21 g (45%) (Found: C, 46.6; H, 3.05; N, 14.65. $C_{37}H_{32}N_{10}Cl_2O_{10}Ru$ requires: C, 46.85; H, 3.15; N, 14.75%). ν/cm^{-1}(KBr) 3400 (br), 3050, 1625, 1590, 1460, 1440, 1415, 1280, 1100 (br), 770, 740, 730 and 620. ^{1}H NMR $[(CD_3)_2SO]$: δ 4.30 (1H, br), 5.55 (1H, t), 6.94 (1H, t), 7.24 (1H, t), 7.45 (4 h, m), 7.50 (1H, d), 7.57 (1H, t), 7.66 (2H, t), 7.68 (2H, d), 7.73 (1H, d), 7.78 (1H, d), 7.82 (1H, s), 7.96 (1H, t), 8.03 (1H, t), 8.07 (2H, t), 8.20 (1H, t), 8.71 (1H, d), 8.75 (1H, d), 8.80 (2H, d), 14.23 (1H, b).

$[(bipy)_2Ru(Hpzbzim)]\cdot 2H_2O$ 5. To a methanol solution (30 cm^3) of **4** (0.19 g, 0.2 mmol) was added a piece of freshly cut sodium metal (*ca.* 0.3 g). The solution changed immediately from red–orange to violet and during stirring for a few minutes the crystalline product began to separate out. The compound was collected by filtration, washed with water and dried under vacuum. It was recrystallized from acetonitrile; yield 0.12 g (80%) (Found: C, 59.6; H, 3.9; N, 18.9. $C_{37}H_{30}N_{10}O_2Ru$ requires: C, 59.45; H, 4.0; N, 18.75%). ν/cm^{-1}(KBr) 3400 (br), 1600, 1565, 1455, 1440, 1415, 1370, 1320, 1270, 1050, 1015, 750 and 730. ^{1}H NMR $[(CD_3)_2SO]$: δ 5.4 (1H, d), 6.47 (1H, t), 6.76 (1H, t), 7.08 (2H, m), 7.18 (1H, s), 7.40 (4H, m), 7.48–7.53(3 H, br), 7.85–7.98 (7H, br), 8.11 (1H, t), 8.63 (3H, d), 8.73 (1H, d), 11.96 (1H, br).

Physical measurements

The C, H and N analyses were performed in-house on a Perkin-Elmer 2400II elemental analyzer. Infrared spectra were recorded on a Perkin-Elmer 783 spectrophotometer using KBr discs and ^{1}H and $\{^1H–^1H\}$COSY NMR spectra on a Bruker Avance DPX300 spectrometer using $(CD_3)_2SO$ solutions.

The electrochemical measurements were carried out with a BAS 100B electrochemistry system. A three-electrode assembly (BAS) comprising a Pt (for oxidation) or glassy carbon (for reduction) working electrode, Pt auxiliary electrode, and an aqueous Ag–AgCl reference electrode were used. The cyclic

voltammetric (CV) and differential pulse voltammetric (DPV) measurements were carried out at 25 °C in acetonitrile solution of the complexes (*ca.* 1 mmol dm^{-3}) and the concentration of the supporting electrolyte tetraethylammonium perchlorate (teap) was maintained to 0.1 mol dm^{-3}. The reference electrode was separated from the bulk electrolyte by a salt bridge containing 0.1 mol dm^{-3} teap in acetonitrile–water (1:1) with the help of a Vycor and heat-shrinkage tubing. The potentials recorded were automatically compensated for *iR* drop in the cell. Under the experimental condition used the reversible oxidation of ferrocene occurred at 0.36 V.

For the variable-pH electrochemical measurements 3:2 acetonitrile–aqueous solutions of the complexes were used. The pH measurements were made with a Beckman Research Model pH meter in combination with a glass-calomel electrode assembly. As the pH meter responded reproducibly to the variation of hydrogen ion concentrations in the above solvent mixture, the 'apparent' pH values obtained directly from the meter readings were referred to as pH. The $E_{\frac{1}{2}}$ value of the ferrocene/ferrocenium couple in acetonitrile–aqueous buffer (pH ≈ 7) medium was found to be 0.26 V.

Electronic spectra were recorded on Shimadzu UV-2100 and Hitachi U3400 spectrophotometers over the UV–VIS and near-IR regions. The spectrophotometric titrations were carried out with a series of acetonitrile–water (3:2) solutions containing the same amount (10^{-5} mmol dm^{-3}) of a complex species and buffer solutions were added to adjust pH in the range 2–12, keeping the ratio of acetonitrile to water (3:2) fixed. The chemical oxidation of the complexes were followed spectrophotometrically by incremental addition of an acidic solution of ceric(IV) ammonium nitrate in acetonitrile–water (3:2) to a solution of the complex in the same solvent mixture.

Emission spectra were recorded on a F-4500 Hitachi fluorescence spectrophotometer. The spectra at 300 K were obtained either in acetonitrile or in methanol–ethanol (1:4), while at 77 K in methanol–ethanol (1:4) glass. Quantum yields of the complexes were determined by a relative method using $[Ru(bipy)_3]^{2+}$ in the same solvent mixture as the standard.[22] Equation (1) was used to calculate the quantum yield,[23] where φ

$$\varphi = \varphi_{std}(A_{std}/A)(I/I_{std})(\eta^2/\eta^2_{std}) \quad (1)$$

and φ_{std} are the quantum yields of unknown and standard samples, A and A_{std} (A_{std} <0.1) are the absorbances at the excitation wavelength, I and I_{std} are the integrated emission intensities and η and η_{std} are the refractive indices of the solutions.

Crystallography

Crystals suitable for structure determination of $[(bipy)_2Ru(pzbzth)Ru(bipy)_2][ClO_4]_3\cdot H_2O$ **3** were obtained by diffusing diethyl ether into a solution of the compound in acetonitrile–methanol (1:1). Intensity data were collected with a Siemens R3m/V diffractometer at 293 K using graphite-monochromated Mo-Kα radiation ($\lambda = 0.71073$ Å). Pertinent crystallographic data are summarized in Table 1. The cell parameters were obtained by least-squares refinement of twenty automatically centred reflections. The standard reflections were monitored after every 150 during data collection and no significant variations in intensities were observed. The intensity data were corrected for Lorentz-polarization effects and semi-empirical absorption correction was made from ψ-scans. A total of 14691 reflections were collected in the θ range 1.63–27.57° with $-14 \le h \le 14$, $0 \le k \le 54$ and $0 \le l \le 17$, of which 14137 ($R_{int} = 0.0879$) reflections were used for structure determination and 734 parameters were refined.

The structure was solved by direct and Fourier methods and refined by full-matrix least squares based on F^2 using the programs SHELXTL-PLUS[24] and SHELXL-93.[25] Neutral atom scattering factors were taken from Cromer and Waber.[26] The non-hydrogen atoms were refined anisotropically, while the hydrogen atoms were placed at the geometrically calculated positions with fixed isotropic thermal parameters. All three perchlorate anions were found to be disordered. As a result, the cation refined smoothly but the R values were rather unsatisfactory. The final least-squares refinement converged to $R1[I > 2\sigma(I)] = 0.107$ based on 5026 'observed' reflections and $wR2 = 0.323$ based on all data. The goodness-of-fit (S) on F^2 was 0.992 and the maximum and minimum peak on the final difference Fourier map corresponded to 1.630 and 0.873 e $Å^{-3}$, respectively.

CCDC reference number 186/1288.

See http://www.rsc.org/suppdata/dt/1999/719/for crystallographic files in .cif format.

Table 1 Crystallographic data for $[(bipy)_2Ru(pzbzth)Ru(bipy)_2][ClO_4]_3\cdot H_2O$ **3**

Formula	$C_{57}H_{43}Cl_3N_{12}O_{13}Ru_2S_2$
M	1476.6
Crystal colour	Dark red
Crystal size/mm	0.43 × 0.35 × 0.28
Crystal system	Monoclinic
Space group	$P2_1/c$
a/Å	11.489(5)
b/Å	41.65(2)
c/Å	13.086(4)
β/°	91.60(2)
U/Å^3	6260(5)
Z	4
D_c/g cm^{-3}	1.567
Scan mode	$\omega/2\theta$
μ(Mo-Kα)/mm^{-1}	0.749
F(000)	2976
$2\theta_{max}$/°	55
Reflections measured	14691
Unique reflections	14137
Parameters refined	734
Final R indices [$I > 2\sigma(I)$]	$R1$ [a] = 0.1073, $wR2$ [b] = 0.2883
R indices (all data)	$R1$ = 0.2109, $wR2$ = 0.3827
S [c]	0.992

[a] $R1(F) = \Sigma||F_o| - |F_c||/\Sigma|F_o|$. [b] $wR2(F^2) = [\Sigma w(F_o^2 - F_c^2)^2/\Sigma w(F_o^2)^2]^{\frac{1}{2}}$. [c] $S = [\Sigma w(F_o^2 - F_c^2)^2/(N-P)]^{\frac{1}{2}}$ where N is the number of data and P the total number of parameters refined.

Results and discussion

Synthesis

The dinuclear complex cation $[(bipy)_2Ru(pzbzth)Ru(bipy)_2]^{3+}$, $\mathbf{3}^{3+}$, was prepared *via* the formation of the mononuclear species $[(bipy)_2Ru(Hpzbzth)]^{2+}$, $\mathbf{1}^{2+}$. Treatment of $[Ru(bipy)_2Cl_2]$ with $Ag[ClO_4]$ in ethanol generates $[Ru(bipy)_2(EtOH)_2]^{2+}$, which on reaction with 1 equivalent of Hpzbzth under weakly acidic conditions produces $\mathbf{1}^{2+}$. A stoichiometric reaction involving $\mathbf{1}^{2+}$, $[Ru(bipy)_2(EtOH)_2]^{2+}$ and triethylamine leads to the formation of $\mathbf{3}^{3+}$. As an alternative approach, $[(bipy)_2Ru(H_3pzbzim)]_2^{2+}$, $\mathbf{4}^{2+}$, was prepared by reacting $H_3pzbzim$ directly with $[Ru(bipy)_2Cl_2]$. However, compared to $\mathbf{1}^{2+}$, the formation of $\mathbf{4}^{2+}$ took a considerably longer period.

Hpzbzth in solution can exist, in principle, as the rotamers **I**–**III**. Consequently, there are three possible ways of binding of the ligand anion with ruthenium(II) by invoking the coordination sites (N⌒N–N⌒N), $(S^{\frown}N–N^{\frown}N)^-$ or $(S^{\frown}N–N^{\frown}S)^-$ to form the dinuclear complex species. We have been able to isolate only one of the linkage isomers, **3**, the crystal structure of which reveals that all the nitrogen atoms are bound to the metal centres. It appears that the exclusive formation of **3** from rotamer **I** is a sequel to the availability of a pathway for delocalization of the double bonds.

Crystal structure

$[(bipy)_2Ru(pzbzth)Ru(bipy)_2][ClO_4]_3\cdot H_2O$ 3. A PLUTO[27]

Table 2 Selected bond lengths (Å) and angles (°) for compound **3**

Ru(1)–N(1)	2.042(11)	Ru(2)–N(7)	2.047(10)
Ru(1)–N(2)	2.068(10)	Ru(2)–N(8)	2.040(9)
Ru(1)–N(3)	2.053(10)	Ru(2)–N(9)	2.055(10)
Ru(1)–N(4)	2.030(11)	Ru(2)–N(10)	2.075(9)
Ru(1)–N(5)	2.115(9)	Ru(2)–N(11)	2.101(9)
Ru(1)–N(6)	2.149(10)	Ru(2)–N(12)	2.128(10)
Ru(1)···Ru(2)	4.723(3)		
N(1)–Ru(1)–N(2)	79.8(4)	N(7)–Ru(2)–N(8)	79.0(4)
N(1)–Ru(1)–N(4)	97.2(5)	N(7)–Ru(2)–N(9)	97.0(4)
N(1)–Ru(1)–N(3)	174.8(4)	N(7)–Ru(2)–N(10)	174.1(4)
N(1)–Ru(1)–N(5)	95.8(4)	N(7)–Ru(2)–N(11)	96.5(4)
N(1)–Ru(1)–N(6)	86.1(4)	N(7)–Ru(2)–N(12)	90.3(4)
N(2)–Ru(1)–N(3)	96.4(4)	N(8)–Ru(2)–N(10)	95.4(4)
N(2)–Ru(1)–N(4)	82.8(4)	N(8)–Ru(2)–N(9)	80.9(3)
N(2)–Ru(1)–N(5)	174.1(4)	N(8)–Ru(2)–N(11)	172.6(4)
N(2)–Ru(1)–N(6)	105.0(4)	N(8)–Ru(2)–N(12)	106.9(3)
N(3)–Ru(1)–N(4)	78.8(5)	N(9)–Ru(2)–N(10)	80.1(4)
N(3)–Ru(1)–N(5)	87.8(4)	N(9)–Ru(2)–N(11)	93.9(3)
N(3)–Ru(1)–N(6)	98.3(4)	N(10)–Ru(2)–N(11)	88.9(3)
N(4)–Ru(1)–N(5)	93.9(4)	N(10)–Ru(2)–N(12)	93.2(4)
N(5)–Ru(1)–N(6)	78.4(4)	N(11)–Ru(2)–N(12)	78.8(4)
N(4)–Ru(1)–N(6)	172.0(4)	N(9)–Ru(2)–N(12)	170.3(4)

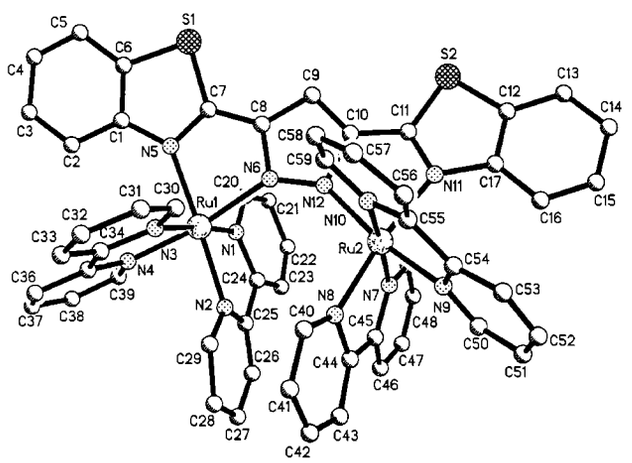

Fig. 1 PLUTO diagram of the $[(bipy)_2Ru(pzbzth)Ru(bipy)_2]^{3+}$ cation in **3**.

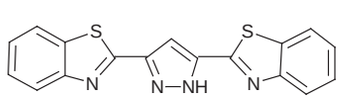

I

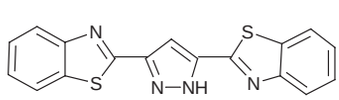

II

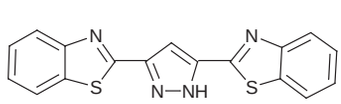

III

diagram of the cation in **3** is shown in Fig. 1 along with atom-labelling. Selected bond distances and angles are given in Table 2. The structure consists of two hexa-coordinated ruthenium(II) centres in which the two $Ru(bipy)_2$ units are bridged by the N(6) and N(12) nitrogen atoms of the pyrazolate moiety of pzbzth anion, while the remaining sixth coordination sites are occupied by the benzthiazole nitrogens N(5) and N(11). Considering the *trans* bipy sites N(1) and N(3) as the major axis for the octahedron due to Ru(1), the equatorial plane is described by N(2), N(4), N(5) and N(6) atoms. Similarly, for Ru(2), the bipy nitrogens N(7) and N(10) are *trans* axial with respect to the plane N(8)–N(9)–N(11)–N(12). In both the metal centres the pyridine nitrogens of each bipy ligand are alternately arranged axially and equatorially. For example, in Ru(1), N(1) is axial and N(2) equatorial. The Ru centres are only slightly displaced from their respective mean planes in the opposite direction by −0.025(1) Å [for Ru(1)] and 0.011 Å [for Ru(2)]. The principal ligand (pzbzth) is generally planar, but there is a twist about the central pyrazolate moiety. The extent of this twist is given by the dihedral angle between the planes C(1)–C(2)–C(3)–C(4)–C(5)–C(6)–S(1)–C(7)–N(8) and C(12)–C(13)–C(14)–C(15)–C(16)–C(17)–N(11)–C(11)–S(2), which is 21.3°. The stereochemical configurations at the two metal sites, however, are not identical due to the difference in distortions of the rings. The distortions of the metal centres from idealized octahedral geometry are reflected in the *cisoidal* angles, which vary from 78.4(4) to 105.0(4)° for Ru(1) and 78.8(4) to 106.9(4)° for Ru(2). The Ru–N bond distances lie in the range 2.030(11)–2.149(10) Å, of which the Ru–N(pyrazolate) distances [Ru(1)–N(6) 2.149(10) Å and Ru(2)–N(12) 2.128(10) Å] and the Ru–N(benzthiazole) distances [Ru(1)–N(5) 2.115(9) Å and Ru(2)–N(11) 2.101(9) Å)] are considerably longer compared to those of the Ru–N(bipy) distances [2.030(11)–2.075(9) Å]. The above bond distances are consistent with σ/π donor characteristic of the bridging ligand. The non-bonding Ru(1)···Ru(2) distance in the compound is 4.723(3) Å. There are no intermolecular contacts exceeding van der Waals' forces.

Table 3 ^{1}H NMR data[a] for $[(bipy)_2Ru(pzbzth)Ru(bipy)_2][ClO_4]_3\cdot H_2O$ **3** in $(CD_3)_2SO$ solution

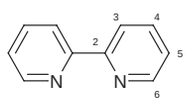

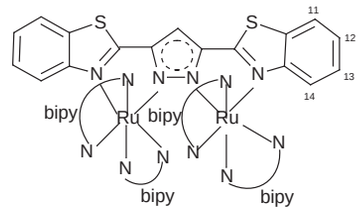

H(7)	8.92(s)		1H	H(13)	7.00(t)	7.7	2H
H(11)	8.26(d)	8.7	2H	H(14)	5.65(d)	8.5	2H
H(12)	7.36(t)	7.7	2H				
bpy ligands							
H(3)	8.00(d)	8.3	2H	H(5)	6.87(t)	7.0	2H
	8.40(d)	8.2	2H		7.36(t)	6.9	2H
	8.46(d)	8.3	4H		7.55(t)	6.8	2H
					8.11(t)	7.0	2H
H(4)	7.36(t)	7.7	2H	H(6)	6.33(d)	5.1	2H
	7.65(t)	7.9	2H		6.85(d)	5.3	2H
	8.00(t)	7.9	4H		7.52(d)	5.0	2H
					8.26(d)	5.7	2H

[a] For ^{1}H NMR data respectively. δ/ppm (multiplicity), J/Hz and number of protons.

^{1}H NMR spectra

The ^{1}H NMR spectral data of complexes **1**–**5** in $(CD_3)_2SO$ solutions are given in the Experimental section. The occurrence of several overlapping resonances in the mononuclear complexes have rendered their assignments rather uncertain. On the other hand, the spectral assignments made for the dinuclear complex **3**, as given in Table 3, could be done straight forwardly from the 2D spectrum shown in Fig. 2. As may be seen from the structure of **3**, the benzothiazole H(14) protons (see Table 3 for proton labelling) would experience maximum shielding by the anisotropic ring current effect of the adjacent bipyridine. Accordingly, the doublet observed at δ 5.65 is assigned to H(14). A triplet observed at δ 7.00 with its cross-peak at δ 5.65 is assignable to H(13) and another triplet observed at δ 7.36 can be attributed to H(12) since it is correlated with both H(13) and H(11); the last one is observed as a doublet at δ 8.26.

Table 4 Electrochemical data for the ruthenium(II) complexes

	Oxidation (CV)				Reduction (DPV)		
	$E_2^{ox}(1)$/V	$\Delta E_p(1)$/mV[a]	$E_2^{ox}(2)$/V	$\Delta E_p(2)$/mV[a]	$E_2^{red}(1)$/V	$E_2^{red}(2)$/V	$E_2^{red}(3)$/V
$[(bipy)_2Ru(Hpzbzth)][ClO_4]_2\cdot 3H_2O$ **1**	1.09	68			−1.46	−1.70	
$[(bipy)_2Ru(pzbzth)][ClO_4]\cdot 2H_2O$ **2**	0.87	61			−1.43	−1.68	
$[(bipy)_2Ru(pzbzth)Ru(bipy)_2][ClO_4]_3\cdot H_2O$ **3**	1.16	62	1.42	65	−1.37[b]	−1.75	−1.86
$[(bipy)_2Ru(H_3pzbzim)][ClO_4]_2\cdot 2H_2O$ **4**	0.89	65			−1.62	−1.90	
$[(bipy)_2Ru(Hpzbzim)]\cdot 2H_2O$ **5**	0.70	125			−1.65	−1.92	

[a] At a scan rate of 100 mV s^{-1}. [b] Two-electron reduction.

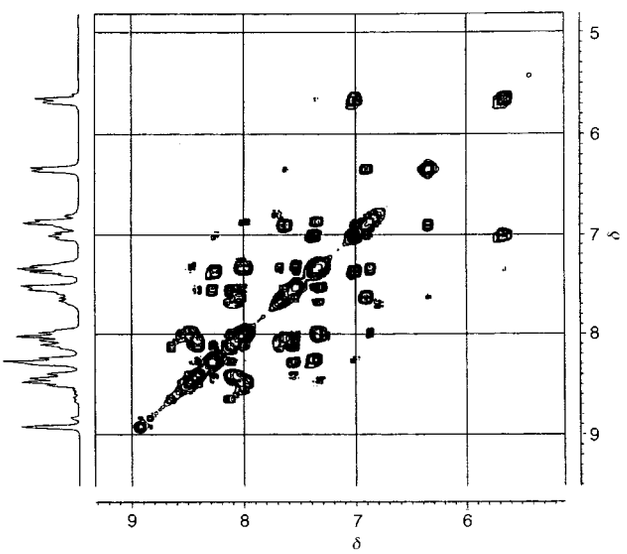

Fig. 2 $\{^1H–^1H\}$ COSY spectrum of **3** in $(CD_3)_2SO$.

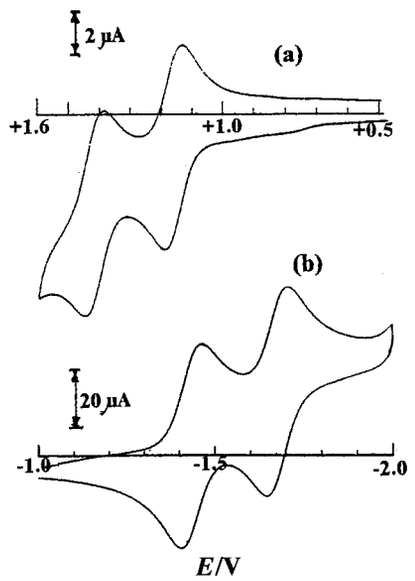

Fig. 3 Cyclic voltammograms of **3** showing oxidation (a) and **1** showing reduction (b) processes in acetonitrile.

The assignment of the bipyridine proton resonances have been made by taking into consideration several generally observed facts,[28] *viz*. the chemical shifts decrease in the order H(3) > H(4) > H(5) > H(6); the H(3) and H(6) protons are observed as doublets, while the H(4) and H(5) protons appear either as a triplet or doublet of doublet; the magnitude of couplings are $J_{3,4}$ and $J_{4,5} \approx 8$ Hz, $J_{5,6} \approx 5$Hz and $J_{3,5}$ and $J_{4,6} \approx 1.2$ Hz. Table 3 summarizes the spectral features observed for the four pairs of pyridine rings in the cation of **3**.

Of considerable interest is the observation that the pyrazolate CH(7) singlet at δ 8.92 is significantly down field-shifted relative to those of the mononuclear complexes **1** (δ 7.78) and **4** (δ 7.82). Clearly, the proton concerned is depleted of electron density in **3**. To explain this observation, we are tempted to invoke the occurrence of a rather unusual S···H(C)···S interaction in the complex species. However, the crystal structure of **3** indicates that the two S···H distances are each *ca*. 3.20 Å, more than the sum of van der Waals' radii (3.05 Å); which goes against C–H···S hydrogen bonding.[29]

Redox activities

The redox properties of complexes **1**–**5** have been studied in acetonitrile solution and the relevant electrochemical data are given in Table 4. In all the cases metal-centred oxidations take place reversibly, as evidenced from the facts that the peak-to-peak separation of the redox couples ($\Delta E_p = 65 \pm 5$ mV) and the ratio of their peak heights ($i_{pa}/i_{pc} \approx 1$) remain constant with the variation of scan rates (50–500 mV s^{-1}) and the current height shows a linear dependence on the square root of scan rate. The cyclic voltammogram of **3** (Fig. 3) shows that the two metal centres are stepwisely oxidized at 1.16 and 1.42 V.

As should be expected, compared to $[(bipy)_2Ru(Hpzbzth)]^{2+}$, for which $E_2^{ox} = 1.09$ V, the removal of an electron from the metal centre in $[(bipy)_2Ru(pzbzth)]^+$ ($E_2^{ox} = 0.87$ V) is easier. On the other hand, the redox potentials for the binuclear complex cations $[(bipy)_2Ru^{II}(pzbzth)Ru^{II}(bipy)_2]^{3+}$–$[(bipy)_2Ru^{III}(pbzbth)Ru^{II}(bipy)_2]^{4+}$ [$E_2^{ox}(1) = 1.16$ V] and $[(bipy)_2Ru^{III}(pzbzth)Ru^{II}(bipy)_2]^{4+}$–$[(bipy)_2Ru^{III}(pzbzth)Ru^{III}(bipy)_2]^{5+}$ [$E_2^{ox}(2) = 1.42$ V] are shifted to more positive values. Evidently, the removal of an electron from a more positively charged cation is more difficult. Thus, it is easier to oxidize the uncharged complex $[(bipy)_2Ru(Hpzbzim)]^\circ$ ($E_2^{ox} = 0.70$ V) relative to the dicationic species $[(bipy)_2Ru(H_3pzbzim)]^{2+}$ ($E_2^{ox} = 0.89$ V). It is interesting that the oxidation of $[(bipy)_2Ru(Hpzbzth)]^{2+}$ is relatively more difficult ($E_2^{ox} = 1.09$ V) than that of $[(bipy)_2Ru(H_3pzbzim)]^{2+}$ ($E_2^{ox} = 0.89$ V), which is indicative of the fact that Hpzbzth is a weaker σ-donor compared to H_3pzbzim.

For the dinuclear complex **3**, the equilibrium constant K_c for the comproportionation reaction $Ru^{II}Ru^{II} + Ru^{III}Ru^{III} \rightleftharpoons 2Ru^{II}Ru^{III}$ is obtained from the relation $K_c = \exp(nF\Delta E_2^{ox}/RT)$. The value of K_c, 2×10^4 dm^3 mol^{-1} at 300 K, gives a measure of the stability of the mixed-valence species over the homovalent species. It also provides an idea whether the mixed-valence species belongs to class III (valence-delocalized) or class II (valence-trapped) system.[30] For a class II system, the value of K_c exceeds 10^6 dm^3 mol^{-1}.

The electrochemical responses of the complexes in the negative potential regime (up to −2.2 V) are also given in Table 4. As shown in Fig. 3(b) for **1**, all the mononuclear complexes undergo two ligand-based stepwise one-electron reversible reductions. On the other hand, for the dinuclear complex **3** three reduction processes are observed, of which the current height of the first wave is twice that of the second and third, indicating that the first one involves simultaneous transfer of two electrons. A similar observation has been reported for several other anionic bridging ligands.[8,11,13]

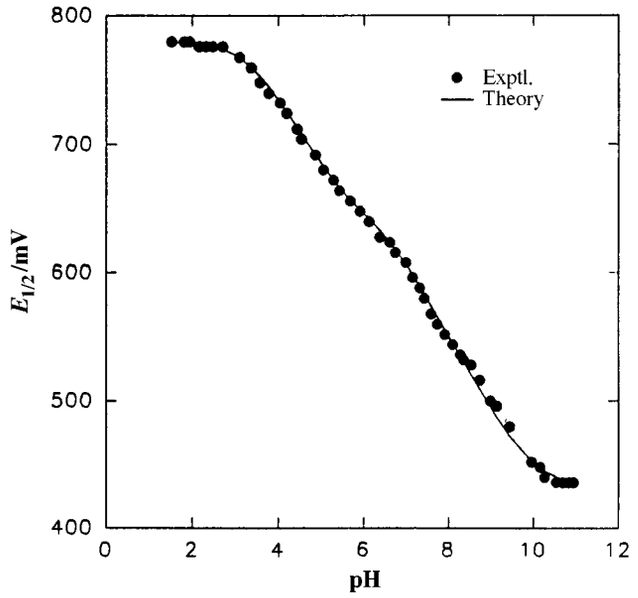

Fig. 4 Variation of the redox potential of the Ru^{II}–Ru^{III} couple in **4** as a function of pH in acetonitrile–water (3:2).

Equilibrium constants involving coupled electron and proton transfer reactions

Since the mononuclear complex $[(bipy)_2Ru(H_3pzbzim)]^{2+}$ contains three azole protons, their stepwise dissociation will substantially affect the redox activities of the resulting complex species. Of the three protons, the pyrazolyl NH should dissociate first and the imidazolyl NH farthest from the metal centre should be least acidic. The redox activity of the complex in acetonitrile–water (3:2), has been monitored over the pH range 1–12. It should be noted that the $E_{\frac{1}{2}}$ values reported here differ from those reported in the preceeding section due to solvent effect. Thus, in pure acetonitrile the $E_{\frac{1}{2}}$ value of ferrocene is 0.36 V, while in acetonitrile–water (3:2) it is 0.26 V.

Fig. 4 shows the variation of $E_{\frac{1}{2}}$ as a function of pH for **4**. It may be noted that in strongly acidic medium, up to pH 2, and in strongly basic medium, pH > 10, the $E_{\frac{1}{2}}$ values remain unchanged. In the intermediate range, 2.5 < pH < 10, steady decrease of $E_{\frac{1}{2}}$ with the increase of pH occurs in two steps with a plateau around pH 5.4 to 6.3. In these two regions, the slopes of $E_{\frac{1}{2}}$ *vs.* pH plots are close to -60 mV$(pH)^{-1}$, indicating the occurrence of two coupled one-electron-one-proton transfer processes. The regions showing invariance of $E_{\frac{1}{2}}$ with pH indicate that the electron transfer is not accompanied by proton transfer. The observed electro-protic reactions are illustrated in Scheme 1.

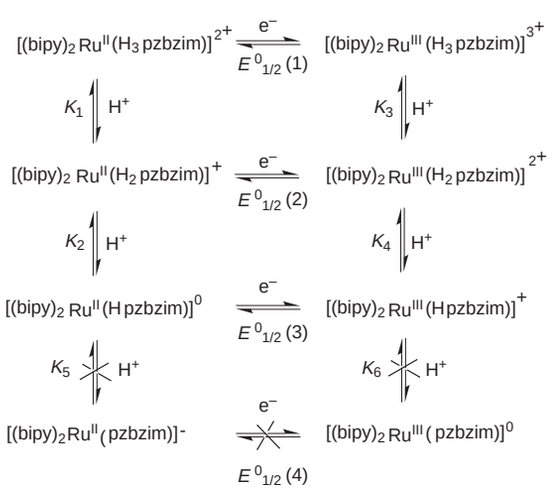

Scheme 1

Table 5 Electronic spectral data for the complexes in acetonitrile

Complex	λ_{max}/nm (ε/dm^3 mol^{-1} cm^{-1})
1	478 (10 790), 438 (11 000), 341 (46 000), 292 (66 000), 232 (54 000)
2	493 (9 800), 458 (10 200), 340 (42 000), 292 (65 000), 232 (52 000)
3	457 (20 100), 425 (22 300), 364 (30 500), 319 (30 700), 287 (95 300), 244 (52 600)
4	502 (9 500), 447 (5 900), 331 (32 100), 311 (50 300), 294 (74 000), 243 (47 000)
5	530 (6 900), 508 (7 000), 352 (33 900), 295 (65 600), 243 (50 100)

As may be noted, K_1 and K_2 are the dissociation constants of the species involving ruthenium(II), while K_3 and K_4 are those of ruthenium(III). Although Scheme 1 includes K_5 and K_6, even at pH 12 there is no sign of dissociation of the benzimidazole proton remote from the metal site.

Inasmuch as the electron transfer reactions under consideration occur reversibly, the observed $E_{\frac{1}{2}}$ can be related to the acid dissociation constants of the complex species by the Nernst equation (2) where $E^{o}_{\frac{1}{2}}$ is the half-wave potential of $[(bipy)_2Ru(H_3pzbzim)]^{2+/3+}$ couple at pH 0. At 25 °C, for $n = 1$ equation (2) reduces to

$$E_{\frac{1}{2}} = E^{o}_{\frac{1}{2}} + \frac{RT}{nF} \ln \frac{[H^+]^2 + K_1[H^+] + K_1K_2}{[H^+]^2 + K_3[H^+] + K_3K_4} \qquad (2)$$

$$E_{\frac{1}{2}} = E^{o}_{\frac{1}{2}} + 0.0591 \log \frac{[H^+]^2 + K_1[H^+] + K_1K_2}{[H^+]^2 + K_3[H^+] + K_3K_4} \qquad (3)$$

A non-linear regression analysis of the $E_{\frac{1}{2}}$ *vs.* pH data provided the acid dissociation constants and redox potentials of the complex species. As shown in Fig. 4, satisfactory simulation of the experimental curve is obtained with $pK_1 = 5.4$, $pK_2 = 10.0$, $pK_3 = 3.0$ and $pK_4 = 6.3$, which vindicates the correctness of Scheme 1.

For the metal-free $H_3pzbzim$, the pK value of the pyrazolyl proton is 10.5, while for the benzimidazolyl protons these are well above 12. By comparison, in the ruthenium(II) complex the pK values for the pyrazolyl and benzimidazolyl protons are 5.4 and 10.0, respectively, and in the corresponding ruthenium(III) species these values are 3.0 and 6.3. Thus, the increase in acidity of the NH protons consequent to the binding of the ligand to the metal centre, especially in the higher oxidation state, is evident. The stepwise dissociation of the ligand protons has the effect of shifting the redox potential $E_{\frac{1}{2}}$ to less positive values from 0.78 to 0.66 to 0.44 V.

The pH-dependant redox behaviour of $[(bipy)_2Ru(Hpzbzth)]^{2+}$ is illustrated in Scheme 2. It should be noted that

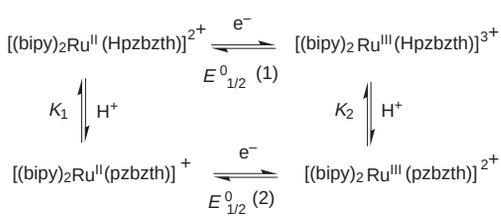

Scheme 2

in this system the pK values of the pyrazolyl proton for the ruthenium(II) species ($pK_1 = 3.5$) and ruthenium(III) species ($pK_2 = 0.7$) are appreciably less compared to those in the earlier discussed system.

Absorption spectroscopic studies

The electronic spectral data of complexes **1**–**5** in acetonitrile are listed in Table 5. All the complexes exhibit two metal-to-ligand

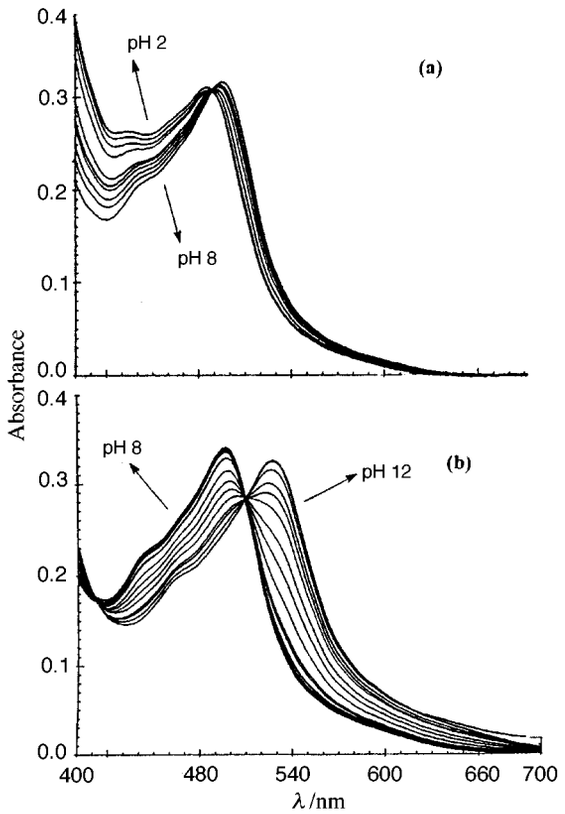

Fig. 5 Changes in the absorption spectra of **4** with the variation of pH in acetonitrile–water (3 : 2). Upper (a) pH 2–8; lower (b) pH 8–12.

$[Ru^{II}(d_\pi) \longrightarrow bpy(\pi^*)]$ charge transfer transitions between 500 and 400 nm and several other intense intraligand π–π* transitions at lower wavelengths.

The influence of pH on the absorption spectral behaviour has been studied for complexes **1** and **4**. The changes that occur for **4** in acetonitrile–water (3 : 2) over the pH range 2–12 are shown in Fig. 5. As may be seen, between pH 2 and 8 the absorption curves pass through an isosbestic point at 490 nm [Fig. 5(a)], while between pH 8 and 12 they pass through the isosbestic point at 505 nm [Fig. 5(b)]. These observations along with the graphical analysis of the spectrophotometric titration data by the method due to Coleman *et al.*,[31] suggest the occurrence of the following acid–base equilibria. The pK values obtained by

$$[(bipy)_2Ru(H_3pzbzim)]^{2+} \overset{K_1}{\rightleftharpoons} [(bipy)_2Ru(H_2pzbzim)]^{+} + H^{+} \quad (4)$$

$$[(bipy)_2Ru(H_2pzbzim)]^{+} \overset{K_2}{\rightleftharpoons} [(bipy)_2Ru(Hpzbzim)] + H^{+} \quad (5)$$

the linear regression analysis of the relation (where A_o and A_f

$$pH = pK_i - \log \frac{A - A_0}{A_f - A_0} \quad (6)$$

are the initial and final absorbances) are $pK_1 = 5.35$ and $pK_2 = 10.00$. These values are in excellent agreement with the results obtained by the electrochemical method ($pK_1 = 5.4$ and $pK_2 = 10.0$).

The deprotonation equilibrium of **1** studied spectrophotometrically (shown in Fig. 6) again reveals the presence of two

$$[(bipy)_2Ru(Hpzbzth)]^{+} \rightleftharpoons [(bipy)_2Ru(pzbzth)]^{+} + H^{+} \quad (7)$$

isosbestic points at 385 and 460 nm. The Coleman plot[28] in this case indicated the presence of two complex species in solution.

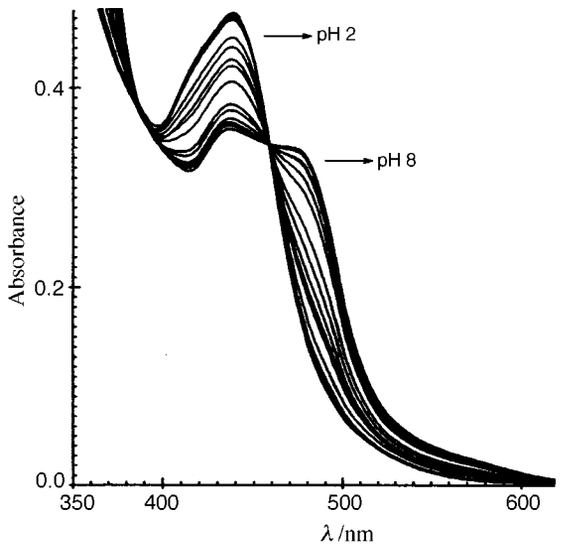

Fig. 6 Changes in the absorption spectrum of **1** with the variation of pH in acetonitrile–water (3 : 2).

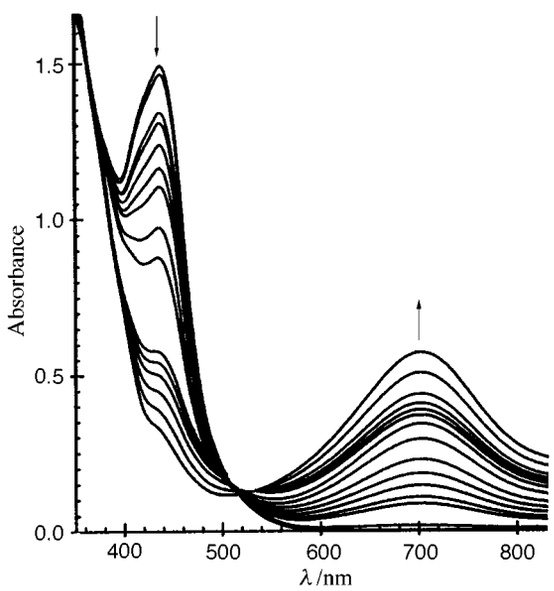

Fig. 7 Changes in the absorption spectrum of **1** on oxidation with cerium(IV) ammonium nitrate in acetonitrile–water (3 : 2).

The pK value thus obtained (3.42), again is in good agreement with the earlier value (3.50).

The redox titrations of **1** and **4** carried out with cerium(IV) ammonium nitrate have also been followed spectrophotometrically. The spectral change that takes place for **1** is shown in Fig. 7. It may be noted that the more intense metal-to-ligand charge transfer (MLCT) band gradually disappears at the expense of the evolution of a less intense ligand to metal charge transfer (LMCT) band. The peak of the LMCT (bridging ligand $\longrightarrow Ru^{III}$) band for **1** and **4** are observed at considerably higher wavelengths, *viz*. 700 and 640 nm, respectively. From the spectrophotometric titrations it became evident that the ruthenium(II) complexes **1** and **4** can be quantitatively oxidized by cerium(IV) to their corresponding ruthenium(III) complexes.

Mixed-valence state

From the electrochemical study of the dinuclear complex **3** it has become apparent that the mixed-valence $[(bipy)_2Ru^{II}(pzbzth)Ru^{III}(bipy)_2]^{4+}$ species has considerable stability in solution with regard to the comproportionation reaction. To obtain more information about the extent of electron delocalization in the mixed-valence state, species $[\mathbf{3}]^{4+}$ has been generated by

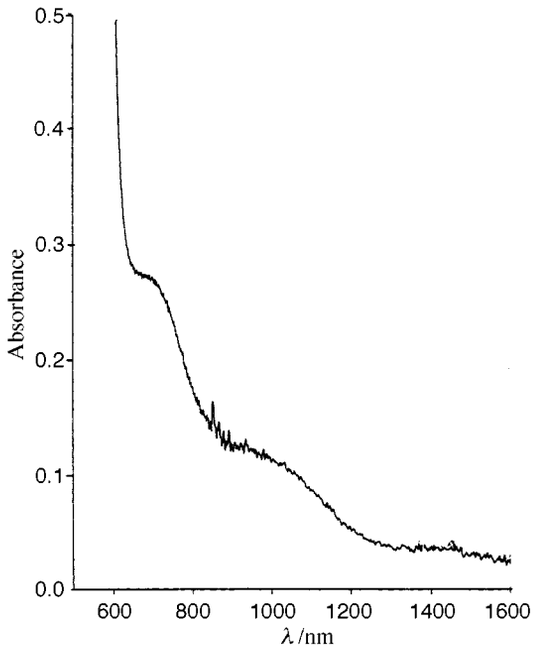

Fig. 8 The intervalence transfer band of $[(bipy)_2Ru^{II}(pzbzth)Ru^{III}(bpy)_2]^{4+}$ in acetonitrile obtained from a (1 : 4) mixture of **3** and $[NH_4]_2[Ce(NO_3)_6]$.

partial chemical oxidation of the diruthenium(II) complex. Fig. 8 shows the absorption spectrum of an acetonitrile solution containing one equivalent each of complex **3** and $[NH_4]_2[Ce(NO_3)_6]$. A new broad absorption band with its peak around 950 cm^{-1} and overlapping with the edge due to the LMCT (ligand $\longrightarrow$ Ru^{III}) transition occurring at 700 nm is observed. The near IR band, which is absent in **3**, is assignable to the intervalence transfer (IT) transition. On deconvolution of the spectrum by Gaussian analysis, the energy of the optical transition (E_{op}) and the bandwidth at half-height ($\Delta\nu_{\frac{1}{2}}$) are obtained as 10500 and 5100 cm^{-1}, respectively. The relatively low molar absorption coefficient of the IT transition (ε_{max} = 110 $dm^3\ mol^{-1}\ cm^{-1}$) indicates that the $Ru^{II}Ru^{III}$ species belongs to a class II system. According to Hush model,[32] for a class II compound the theoretical value of $\delta\nu_{\frac{1}{2}}$ is given by equation (8).

$$\Delta\nu_{\frac{1}{2}} = (2310\ E_{op})^{\frac{1}{2}}\ cm^{-1} \quad (8)$$

The predicted value of $\Delta\nu_{\frac{1}{2}}$ (4930 cm^{-1}) is in good agreement with the observed value (5100 cm^{-1}).

The resonance energy exchange integral or the magnitude of electron coupling between the heterovalent metal centres, H_{AB}, can be obtained from the relation[32,33] where d is the intra-

$$H_{AB} = [2.06 \times 10^{-2}(\varepsilon_{max}\Delta\nu_{\frac{1}{2}}E_{op})^{\frac{1}{2}}]/d \quad (9)$$

molecular metal–metal distance in Å. With d = 4.723 Å, H_{AB} for $[3]^{4+}$ (335 cm^{-1}) is typical of class II $Ru^{II}Ru^{III}$ compounds, which lie in the range 50–700 cm^{-1}.[33,34] The metal–metal interaction in mixed-valence systems would depend on the overlap between the frontier orbitals of the metal and the bridging ligand, which, in turn, would depend on the energy gap between the metal d_π orbitals and the LUMO and HOMO orbitals of the bridging ligand.

Luminiscence spectra

The emission spectral behaviour of complexes **1**–**4** have been studied at 300 K in acetonitrile and methanol–ethanol (1 : 4) solutions and at 77 K in methanol–ethanol (1 : 4) glass. Table 6 summarizes excitation wavelength, emission peak and quantum yield (at 300 K). For all the complexes, when any of the two MLCT bands are excited, emission spectral features remain unchanged. The spectra recorded in methanol–ethanol solution are of better quality compared to those obtained in acetonitrile. The luminiscence spectra of **1** and **3** in frozen glass are shown in Fig. 9. The observed spectra have the feature characteristic of emission from triplet MLCT excited state, which corresponds to spin forbidden ruthenium(II) $\longrightarrow$ bipy transition.[34]

Table 6 Emission spectral data of the complexes in methanol–ethanol (1 : 4)

Complex	λ_{ex}/nm	λ_{em}/nm		$10^3\ \varphi$ (300 K)
		300 K	77 K	
1	478, 438	630	610	2.4
2	493, 458	650	615	3.6
3	457, 425	630	610	3.0
4	502, 447	680	640	3.5

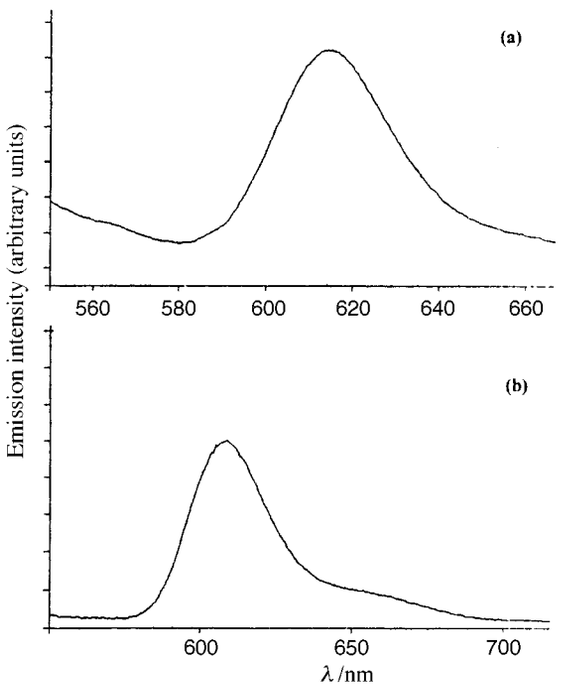

Fig. 9 Luminescence spectra of **1**(a) and **3**(b) in methanol–ethanol (1 : 4) frozen glass at 77 K.

Acknowledgements

K. N. is thankful to the Council of Scientific and Industrial Research, India for funding this work.

References

1 V. Balzani, A. Juris, M. Venturi, S. Campagna and S. Serroni, *Chem. Rev.*, 1996, **96**, 759.
2 J.-P. Collin, P. Gavina, V. Heitz and J.-P. Sauvage, *Eur. J. Inorg. Chem.*, 1998, 1; J.-P. Sauvage, J.-P. Collin, J.-C. Chambron, S. Guillerez, C. Coudret, V. Balzani, F. Barigelletti, L. DeCola and L. Flamigni, *Chem. Rev.*, 1994, **94**, 993.
3 M. D. Ward, *Chem. Soc. Rev.*, 1995, 121.
4 G. Giuffrida and S. Campagna, *Coord. Chem. Rev.*, 1994, **135/136**, 517.
5 R. J. Crutchley, *Adv. Inorg. Chem.*, 1994, **41**, 273.
6 A. Harriman and R. Ziessel, *Chem. Commun.*, 1996, 1707.
7 E. C. Constable, *Prog. Inorg. Chem.*, 1994, **42**, 67.
8 R. Have, A. H. J. Dijkhuis, J. G. Haasnoot, R. Prins, J. Reedijk, B. E. Buchanan and J. G. Vos, *Inorg. Chem.*, 1988, **27**, 2185; R. Hage, J. G. Haasnoot, H. A. Nieuwenhuis, J. Reedijk, D. J. A.

Ridder and J. G. Vos, *J. Am. Chem. Soc.*, 1990, **112**, 9245; J. H. van Diemen, R. Hage, J. G. Haasnoot, H. E. B. Lempers, J. Reedijk, J. G. Vos, L. De Cola, F. Barigelletti and V. Balzani, *Inorg. Chem.*, 1992, **31**, 3518; S. Serroni, S. Campagna, G. Denti, T. E. Keyes and J. G. Vos, *Inorg. Chem.*, 1996, **35**, 4513 and references therein.
9 H. P. Hughes and J. G. Vos, *Inorg. Chem.*, 1995, **34**, 4001.
10 D. P. Rillema, R. Sahai, P. Matthews, A. K. Edwards, R. J. Shaver and L. Morgan, *Inorg. Chem.*, 1990, **29**, 167.
11 A. M. Bond and M. Haga, *Inorg. Chem.*, 1986, **25**, 4507; M. Haga and A. M. Bond, *Inorg. Chem.*, 1991, **30**, 475.
12 M. Haga, T. Ano, K. Kano and S. Yamabe, *Inorg. Chem.*, 1991, **30**, 3843; M. Haga, T. Ano, T. Ishizaki, K. Kano, K. Nazaki and T. Ohono, *J. Chem. Soc.*, *Dalton Trans.* 1994, 263.
13 K. Nozaki, T. Ohno and M. Haga, *J. Phys. Chem.*, 1992, **96**, 10880; T. Ohno, K. Nozaki and M. Haga, *Inorg. Chem.*, 1992, **31**, 4256.
14 M. Haga, M. M. Ali, H. Macgawa, K. Nozaki, A. Yoshimura and T. Ohno, *Coord. Chem. Rev.*, 1994, **132**, 99; M. Haga, M. M. Ali and R. Arakawa, *Angew. Chem.*, *Int. Ed. Engl.*, 1996, **35**, 76.
15 J. M. De Wolf, R. Hage, J. G. Haasnoot, J. Reedijk and J. G. Vos, *New. J. Chem.*, 1991, **15**, 501; H. E. B. Lempers, J. G. Haasnoot, J. Reedijk, R. Hage, F. M. Weldon and J. G. Vos, *Inorg. Chim. Acta*, 1994, **225**, 67.
16 D. D. Perrin, W. L. Armarego and D. R. Perrin, *Purification of Laboratory Chemicals*, 2nd edn., Pergamon, Oxford, 1980.
17 H. H. Lee, B. F. Cain, W. A. Denny, J. S. Buckleton and G. R. Clark, *J. Org. Chem.*, 1989, **54**, 428.
18 B. P. Sullivan and T. J. Meyer, *Inorg. Chem.*, 1978, **17**, 3334.
19 D. D. Perrin and B. Dempsey, *Buffers for pH and Metal Ion Control*, Chapman and Hall, London, 1974.
20 A. W. Addison, T. N. Rao and C. G. Wahlgren, *J. Heterocycl. Chem.*, 1983, **20**, 1481.
21 M. A. Phillips, *J. Chem. Soc.*, 1928, 2393.
22 G. A. Crosby and W. H. Elfring, Junior, *J. Phys. Chem.*, 1976, **80**, 2206; M. J. Cook, A. P. Lewis, G. S. G. McAuliffe, V. Sharda, A. J. Thomson, J. L. Glasper and D. J. Robbins, *J. Chem. Soc.*, *Perkin Trans. 2*, 1984, 1293.
23 J. van Houten and R. J. Watts, *J. Am. Chem. Soc.*, 1976, **98**, 4853.
24 G. M. Sheldrick, SHELXTL PLUS Program Package (PC Version), University of Göttingen, 1989.
25 G. M. Sheldrick, SHELXL 93, A Program for Crystal Structure Refinement, Gamma-Test Version, University of Göttingen, 1993.
26 D. T. Cromer and J. T. Waber, *International Tables for X-Ray Crystallography*, Kynoch Press, Birmingham, 1974, vol. 4.
27 PLUTO, W. D. S. Motherwell and W. Clegg, Program for Plotting Molecular and Crystal Structures, University of Cambridge, UK.
28 E. C. Constable and K. R. Seddon, *J. Chem. Soc.*, *Chem. Commun.*, 1982, 34; J. L. Walsch and B. Durham, *Inorg. Chem.*, 1982, **21**, 329; P. J. Steel, F. Lahousee, D. Lerner and C. Marzin, *Inorg. Chem.*, 1983, **22**, 1488; R. Hage, R. Prins, J. G. Haasnoot, J. Reedijk and J. G. Vos, *J. Chem. Soc.*, *Dalton Trans.*, 1987, 1389; J. Bolger, A. Gourdon, E. Ishow and J.-P. Launy, *Inorg. Chem.*, 1996, **35**, 2937.
29 D. Braga, F. Grepioni and G. R. Desiraju, *Chem. Rev.*, 1998, **98**, 1375.
30 M. B. Robin and P. Day, *Adv. Inorg. Chem. Radiochem.*, 1967, **10**, 247.
31 J. S. Coleman, L. P. Varga and S. H. Mastin, *Inorg. Chem.*, 1970, **9**, 1013.
32 C. Creutz, *Prog. Inorg. Chem.*, 1983, **30**, 1.
33 R. J. Crutchley, *Adv. Inorg. Chem.*, 1994, **41**, 273.
34 A. Juris, V. Balzani, F. Barigelletti, S. Campagna, P. Belser and A. von Zelewsky, *Coord. Chem. Rev.*, 1988, **84**, 85.

Paper 8/06989A